Preprints of the 18th IFAC World Congress
Milano (Italy) August 28 - September 2, 2011

Fuel-Efficient Model-Based Optimal MIMO Control for PCCI Engines

P. Drews * **T. Albin** * **F.-J. Heßeler** * **N. Peters** ** **D. Abel** *

* *Institute of Automatic Control, RWTH Aachen University, Aachen, Germany (e-mail: p.drews@irt.rwth-aachen.de)*
** *Institute for Combustion Technology, RWTH Aachen University, Aachen, Germany (e-mail: office@itv.rwth-aachen.de)*

Abstract: Recent research in modern combustion technologies, like partial homogeneous charge compression ignition (PCCI), demonstrates the capability of reducing pollutant emissions, e.g. soot and NO_X. In addition to this advantage, a possibility to reduce fuel consumption and noise production by model-based optimal control is presented in this paper. In order to understand the basic properties of the PCCI mode, process measurements were conducted using a slightly modified series diesel engine. Control variables are engine combustion parameters: the indicated mean effective pressure, the combustion average and the maximum gradient of the cylinder-pressure. Control inputs are the parameters: quantity of injected fuel, start of injection and the intake manifold fraction of recirculated exhaust gas. The process has very fast, almost proportional behaviour over the engine's working cycles. Focusing on the static behaviour of the process, a nonlinear neural network model is used for identification. Successive linearization of the nonlinear network is used to build an affine internal controller model for the actual operating point. The presented controller structure is able to consider constraints by individual formulation of the cost function. With this configuration the closed-loop process is able to track the combustion setpoints with high control quality with minimal possible fuel consumption and combustion noise.

Keywords: Model-based Optimal Predictive control, MIMO, Affine, Automotive control

1. INTRODUCTION

From the political, economic and environmental point of view, further reduction of fuel consumption or CO_2-emission, respectively, is needed to secure long-term operation of combustion engines as drive propulsion systems. In addition, more reduction of pollutant emissions, like soot, nitrogen oxide and unburned hydrocarbons, will be decisive for the future acceptance of diesel engines. These requirements imply higher standards of the actual development of combustion engines and their control. The partial homogeneous charge compression ignition (PCCI), one of the modern combustion methods, is a promising approach to achieve these standards. By improvement of the combustion, the use of expensive additional equipment for exhaust gas aftertreatment can be minimized. Besides, it is more efficient to reduce the production of pollutants during combustion than during an inefficient exhaust gas aftertreatment. Recent research has provided many basic principles concerning the low temperature combustion (for a detailed overview see Yao et al. (2009)). Because of the early injection, it is not possible to define the start of combustion of the partially homogenized air-fuel mixture, furthermore the combustion process is unknown. Here, at least a feed forward control is required to adjust the control inputs to get a necessary position of the combustion average CA50, where 50 % of the injected fuel is consumed during combustion. The engine combustion process is influenced by many actuator inputs and immeasurable disturbances. Therefore, the limit of the capabilities of a pure feedforward control without feedback can be exceeded. There are only a few published approaches concerning intelligent model-based MIMO-control of the low-temperature engine combustion. The majority of these approaches use, in contrast to the control presented in this contribution, a variable valve timing as control input, e.g. Bengtsson et al. (2006) and Shaver (2009). This offers a high degree of freedom which can be very complex from control point of view.

The integration of a feedback in a control structure requires the measurement of important combustion parameters like the indicated mean effective pressure IMEP, the position of the combustion average and the maximum cylinder pressure gradient dpmax. The cylinder pressure gradient correlates with the combustion noise emission of the engine. To obtain these values, the measurement of the cylinder pressure and its real-time analysis is used. In combination with the control inputs, which are fuel mass injected (FMI), start of injection (SOI) and the fraction of exhaust gas recirculated (X_{EGR}), the resulting control problem has a coupled MIMO (Multiple Input Multiple Output) structure, which is controlled by a model-based optimal controller. This controller is able to consider an individually formulated cost function. For example, the control problem is constrained by the minimization of the quantity of injected fuel by penalizing high amounts of FMI in the costs. Also, additional constraints like the minimization of pollutants in the exhaust gas are possible.

The work presented in this paper is based on the results shown in Drews et al. (2010). Here, the control is improved by adding constraints for realizing a control for a fuel efficient engine with minimized noise emissions. It is organized as follows. First, the reasons for implementation of the PCCI combustion are given. To understand the relationships between control inputs and control outputs, measurements using a real engine are presented. The next step is the process identification to build up a nonlinear model. This model is the basis for generating a successively updated affine internal controller model. Using this model, the structure of the optimal controller is described. Finally, validations by means of experimental closed loop simulations are made.

2. MIMO CONTROL PROBLEM

2.1 PCCI - Partial Homogenized Charge Compression Ignition

Reduction of pollutant emissions is the main motivation for the development of alternative combustion methods. The conflict of aims between production of soot and nitrogen oxide of the classic diesel engine is caused by the heterogeneous air/fuel mixture formation. Fig. 1 shows the areas of NO_X and soot production depending on local combustion temperatures and local air/fuel mixtures λ, Mollenhauer and Tschoeke (2007). Because of the fuel injection at very high pressures and small ignition delays, there are very high mixture gradients during combustion in the classical stratified mode of a conventional diesel engine (DI-Diesel). Its operation area (dashed line) is very large and extends widely into the areas at which soot and NO_X production take place. By shifting the start of injection to earlier times, the ignition delay is extended and thus more time for a partial (PCCI) or full (HCCI) homogenization of the mixture is available. Hence, rich mixtures $\lambda < 0.8$ are avoided, and, therefore, no soot is produced. In case of full homogenization, the possible range of local λs is very low. To avoid NO_X formation, the local temperature is decreased by a higher EGR-fraction. An alternative way to lower the thermal levels is to decrease the compression ratio $\epsilon = (V_D + V_C)/V_C$ (V_C: cylinder volume when piston at top dead center, V_D displacement of cylinder) of the engine for PCCI/HCCI mode. Unfortunately, there is a disadvantage to the mentioned methods to obtain low temperature combustion, which has to be taken into account when promoting this modern kind of engine combustion. By decreasing the local temperature, it may be, that the operation area is shifted to the limit of complete combustion. The position of this limit depends on the engine operation point (speed and load) and the combustion process. It can be placed somewhere in between 1300K<T<1400K, Dec (2009). Hence, when reaching this area, the combustion stops locally, and the amount of unburned hydrocarbons (HC) and carbon monoxide (CO) in the exhaust gas increases. It is a big challenge for future research to avoid this area in PCCI combustion.

To get an optimal process management, combustion parameters, which result from the analysis of the cylinder pressure, are used as control outputs. These are the indicated mean effective pressure, the combustion average and the maximum gradient of the cylinder pressure.

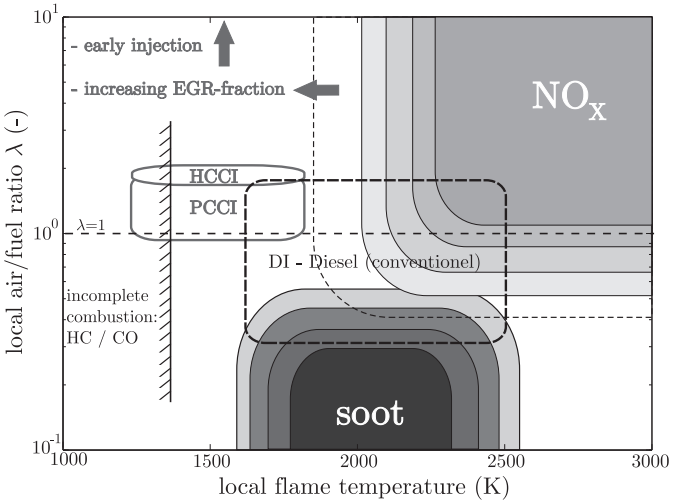

Fig. 1. Areas of NO_X and soot production over local flame temperature and λ with DI/HCCI/PCCI operation areas, Mollenhauer and Tschoeke (2007), Dec (2009)

The start of injection, the quantity of injected fuel and the intake manifold fraction of recirculated exhaust gas ($X_{EGR} = \dot{M}_{EGR}/(\dot{M}_{EGR} + \dot{M}_{Air})$ with $\dot{M}_{Air}$ as fresh air mass flow, $\dot{M}_{EGR}$ as the mass flow of recirculated exhaust gas) are taken as control inputs. In this paper, the focus in controller development is on PCCI mode instead of HCCI mode. The PCCI mode combines the benefits of the full HCCI mode with the benefits of the stratified mode Yao et al. (2009), Kanda et al. (2005). With respect to combustion control, PCCI also has advantages compared to HCCI. SOI determines the degree of homogenization and influences the combustion indirectly. In order to have a permanent influence of SOI especially on the combustion timing, the full homogeneous mode (HCCI) is avoided due to limitation of the lower boundary of SOI: keeping its operation range approximately between -50 and -10 °CA aTDC, it is possible to realize a partial homogenized mixture. This range of SOI and EGR-fractions $X_{EGR} > 20\%$, roughly define the conditions for PCCI combustion at the studied engine.

2.2 Measurement of the PCCI process

An automotive 1.9 l four-cylinder diesel engine with a common rail injection was used for all experiments. The engine is equipped with external exhaust gas recirculation and a turbocharger with a variable geometry turbine. The dedicated model-predictive control for the air path, which adjusts the demanded air mass flow and boost pressure, is presented in Drews et al. (2009). According to the statements made in subsection 2.1, to enhance the PCCI mode, the original compression ratio $\epsilon = 17.5$ is lowered to $\epsilon = 15$, similar to the approach presented in Kim and Lee (2007). To avoid too much fuel-wall interactions caused in the early injection, the injection pressure is lowered to 700 bar. The injection strategy is single injection for all experiments. Fig. 2 shows the input/output structure of the process. The measured cylinder pressure is interpreted by a hardware for thermodynamic real-time analysis (FI2RE by IAV GmbH), which calculates IMEP, CA50 and dpmax at the end of each combustion cycle. To get an appropriate internal controller model, process identification, which

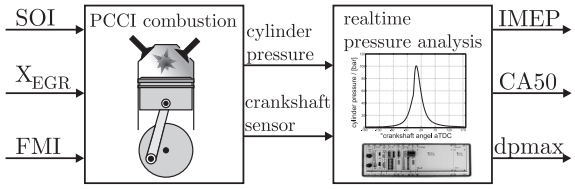

Fig. 2. Inputs and outputs of the PCCI engine and pressure analysis

includes measurements at the test bench, is required. Like already shown in Drews et al. (2010), the dynamic behaviour over the combustion cycles is almost proportional without significant delays and without overshoots in most instances. Therefore, the cycle-to-cycle dynamics of the process will be neglected. Instead, the focus will be set on the static, highly nonlinear behaviour of the PCCI combustion. To identify all relationships, quasi-stationary measurements are carried out. These are realized by very slow variation of SOI of the single injection in the shape of a ramp in the region of -10 to -60 °CA aTDC within a duration of 100 seconds for each ramp. This test is executed for different FMI (10, 12.5, 15, 17.5, 20 mm^3/cycle) at each X_{EGR} $(20\%, 30\%, 40\%, 50\%)$. All in all, 20 measurements have been made with a total recording time of approximately 40 minutes for one engine speed. By linear interpolation between the supporting points of the measurements for each X_{EGR} a dataset for CA50, IMEP and dpmax over the inputs SOI and FMI is obtained. Figs. 3 to 6 show examples of the resulting data for an engine speed of 2000 rpm. Fig. 3 presents a three-dimensional contour plot of a CA50-dataset for X_{EGR}=30%. For all applied FMI, CA50 is shifted, with decreasing SOI, to earlier times until the start of injection is approximately SOI=-45 °CA aTDC. For a very early start of injection, CA50 is shifted to later times. Fig. 4 shows the dataset for IMEP also for X_{EGR}=30%. It can be observed that IMEP increases almost proportional to FMI and remains constant for SOI until -45 °CA aTDC. Fig. 5 displays the maximum pressure gradient dpmax for X_{EGR}=30%. It can be identified that the highest pressure gradients occur in the PCCI area of about SOI=-40 °CA aTDC

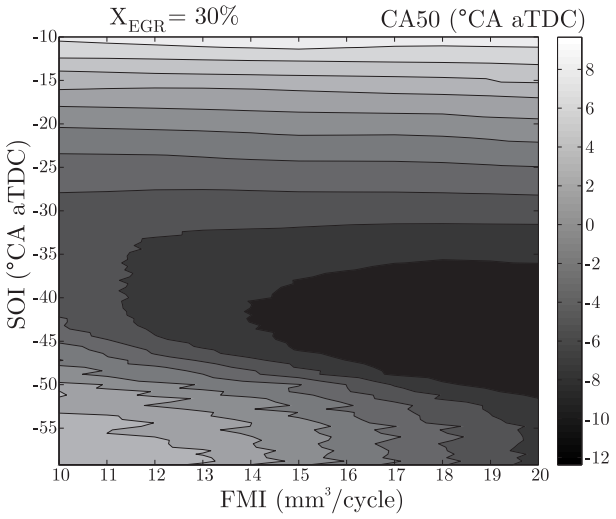

Fig. 3. Combustion average CA50 over quantity of injected fuel FMI and start of injection SOI

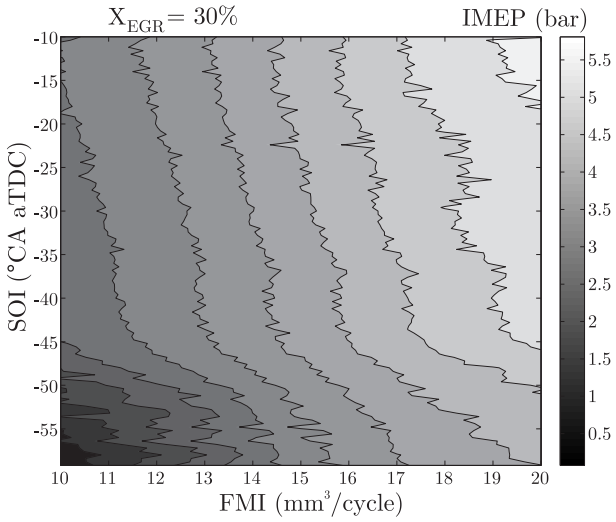

Fig. 4. Indicated mean effective pressure IMEP over quantity of injected fuel FMI and start of injection SOI

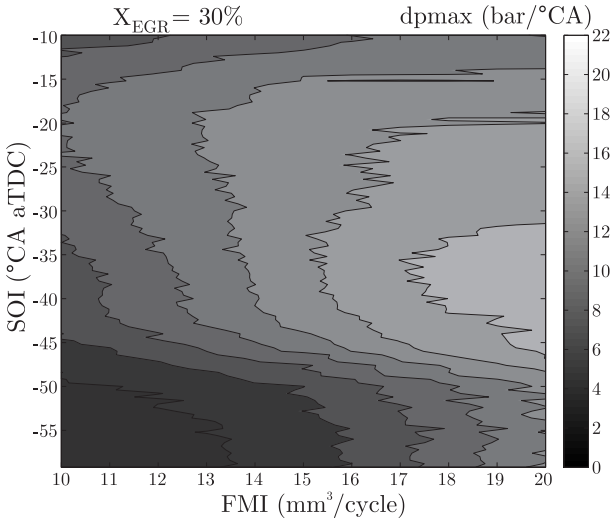

Fig. 5. Maximum pressure gradient dpmax over FMI and SOI

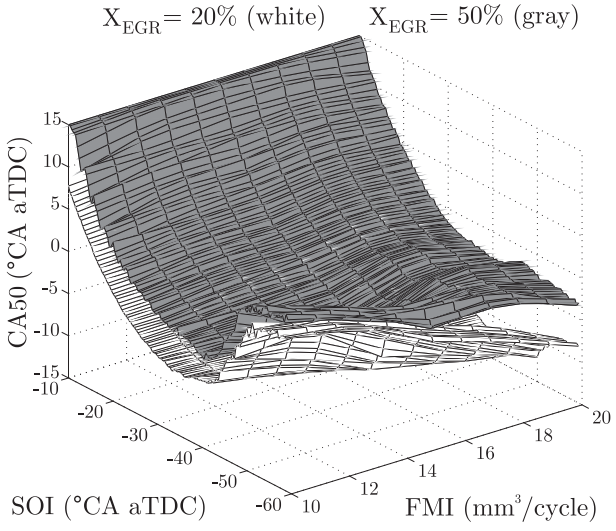

Fig. 6. Comparison of CA50 for X_{EGR} = 20% (white) and X_{EGR} = 50% (gray)

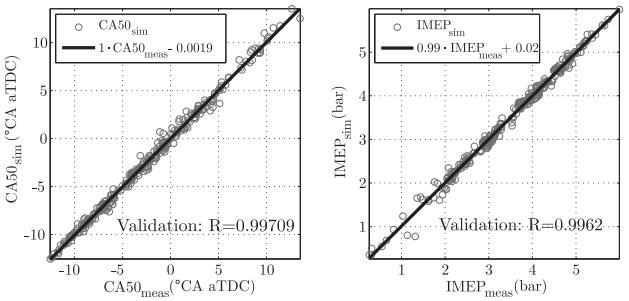

Fig. 7. Validation of the nonlinear ANNs of CA50 and IMEP

and high FMI. To analyze the effects of the increasing EGR-fraction on the position of CA50 in Fig. 6, CA50 for X_{EGR}=20% (white) is compared to X_{EGR}=50% (gray). For all SOI and FMI, the position of the combustion average at X_{EGR}=50% is shifted to later times than the one at X_{EGR}=20%.

2.3 Nonlinear modeling of the PCCI process

The datasets presented in the previous chapter are used for the nonlinear system identification in this paper. Therefore, an artificial neural network (ANN) with sigmoid activation functions and feed forward structure is chosen. In analogy to the datasets, an input vector U and an output function vector f are defined:

$$U = \begin{bmatrix} U_1 \\ U_2 \\ U_3 \end{bmatrix} = \begin{bmatrix} FMI \\ SOI \\ X_{EGR} \end{bmatrix}, \quad f(U) = \begin{bmatrix} f_1(U) \\ f_2(U) \\ f_3(U) \end{bmatrix} = \begin{bmatrix} CA50 \\ IMEP \\ dpmax \end{bmatrix} \quad (1)$$

For a single element $f_j(U)$ in $f(U)$, the ANN can be formulated as:

$$f_j(U) = \Gamma_j + \sum_{i=1}^{n} \left[\left(\frac{2}{1 + e^{-2(\mathbf{\Phi}_{j_{(i,\cdot)}} U + \Xi_{j_i})}} - 1 \right) \Psi_{j_i} \right] \quad (2)$$

with Γ_j as a bias for the output, n the number of neurons, $\mathbf{\Phi}_{j_{(i,\cdot)}}$ as a weight matrix for the input U concerning the neuron i, Ξ_{j_i} as a bias for the exponent and Ψ_{j_i} as a correction factor for the neuron i. The network is trained via scaled conjugate gradient back-propagation. In Fig. 7, a validation result for a neural network, according to (2), is shown with $n = 20$ for CA50 and IMEP. The validation dataset is different to the training dataset. In both cases, the coefficients of correlation R are approximately 1. This shows the desired good correlation between the simulated and the measured data. The resulting regression lines are running nearly through the origin, their slopes are approximately equal to one. The same good correlation results for the identification of dpmax not shown here.

3. OPTIMAL CONTROL STRUCTURE

3.1 Cost Function

To get optimal control input corrections U_{k+1} regarding constraints, like a minimal fuel consumption or minimal noise emission, the following nonlinear quadratic minimization problem is considered:

$$\min_{U_{k+1}} J(f(U_{k+1}), U_{k+1})$$
$$J = \|f(U_{k+1}) - W_{k+1}\|^2_{\mathbf{Q}} + \|U_{k+1} - U_k\|^2_{\mathbf{R}} + \|U_{k+1}\|^2_{\mathbf{P}} \quad (3)$$

with k as the actual and $k+1$ as the upcoming future time step. $f(U_{k+1})$ is the model prediction for the next time step, W_{k+1} is the reference value. $U_{k+1} - U_k$ is the control input correction u_{k+1}:

$$u_{k+1} = U_{k+1} - U_k \quad (4)$$

$\mathbf{Q}, \mathbf{R}$ in the cost function J are weight matrices to adjust the degree of penalization for the control errors and the control input corrections. $\mathbf{P}$ is for optional penalization of the absolute values of the control inputs (e.g. FMI).

3.2 Convex Problem Formulation

For easy analytic minimization, the nonlinear function (3) has to be simplified to a convex formulation. For this formulation $f(U_{k+1})$ in (3) has to be linear or affine, Boyd and Vandenberghe (2004). Therefore, the nonlinear neural network model (2) has to be linearized at the actual operation point. Since the network is static without internal feedback, the linearization only depends on the actual U_k

$$y_{k+1} = \underbrace{\left.\frac{\partial f}{\partial U}\right|_{U_k}}_{\mathbf{K}_k} \cdot u_{k+1} \quad (5)$$

with the deviation variables $y_{k+1} = Y_{k+1} - Y_k$, $u_{k+1} = U_{k+1} - U_k$ and $Y_{k+1} = f(Y_k, U_k, u_{k+1})$. For a single element $f_j(U)$ of $f(U)$, the derivative of (2) is:

$$\left.\frac{\partial f_j}{\partial U}\right|_{U_k} = \begin{bmatrix} K_{j_{FMI}} \\ K_{j_{SOI}} \\ K_{j_{X_{EGR}}} \end{bmatrix} = \mathbf{\Phi}_j^T \begin{bmatrix} \Omega_{j_1} \\ \vdots \\ \Omega_{j_n} \end{bmatrix} \quad (6)$$

where

$$\Omega_{j_i} = \frac{4e^{-2(\mathbf{\Phi}_{j_{(i,\cdot)}} U_k + \Xi_{j_i})}}{\left(1 + e^{-2(\mathbf{\Phi}_{j_{(i,\cdot)}} U_k + \Xi_{j_i})}\right)^2} \cdot \Psi_{j_i}, \quad i = 1...n \quad (7)$$

By calculation of (6) for every j and arranging the resulting $K_{j_{U_{(1..3)}}}$, the gain matrix (Jacobian) yields:

$$\mathbf{K}_k(U_k) = \begin{bmatrix} K_{CA50_{FMI}} & K_{CA50_{SOI}} & K_{CA50_{X_{EGR}}} \\ K_{IMEP_{FMI}} & K_{IMEP_{SOI}} & K_{IMEP_{X_{EGR}}} \\ K_{dpmax_{FMI}} & K_{dpmax_{SOI}} & K_{dpmax_{X_{EGR}}} \end{bmatrix} \quad (8)$$

By using the actual model output $\hat{Y}_k$, the following affine model may be expressed as:

$$\hat{Y}_{k+1} = \hat{Y}_k + \mathbf{K}_k \cdot u_{k+1} \quad (9)$$

Instead of taking the last model value $\hat{Y}_k$, the affine part of the model is replaced by the measurement $\tilde{Y}_k$ of the plant. Thereby, the feed forward structure is complemented by a control with feedback, which is able to compensate for disturbances:

$$Y_{k+1} = \tilde{Y}_k + \mathbf{K}_k \cdot u_{k+1} \quad (10)$$

The model is updated successively by inserting the actual U_k in (7) in every timestep k. Assuming that the affine model (10) is responsible for small deviations from the

actual process state $\tilde{Y}_k$, the cost function can be simplified to a convex formulation:

$$\min_{u_{k+1}} J(u_{k+1})$$
$$J = \|\tilde{Y}_k + \mathbf{K}_k \cdot u_{k+1} - W_{k+1}\|^2_{\mathbf{Q}} + \|u_{k+1}\|^2_{\mathbf{R}} + \|U_k + u_{k+1}\|^2_{\mathbf{P}} \tag{11}$$

3.3 Optimal Control Input Corrections

The aim is to find the global minimum of the convex problem (11). Therefore, the zero of the first derivative (Jacobian) has to be calculated:

$$\frac{dJ}{du_{k+1}} = \left(2(\tilde{Y}_k - W_{k+1})^T \mathbf{Q}\mathbf{K}_k + 2{U_k}^T \mathbf{P}\right)^T + 2({\mathbf{K}_k}^T \mathbf{Q}\mathbf{K}_k + \mathbf{R} + \mathbf{P})u_{k+1} \stackrel{!}{=} 0 \tag{12}$$

with the Hessian matrix $\mathbf{H}$ and the gradient vector g of J

$$\mathbf{H} = 2({\mathbf{K}_k}^T \mathbf{Q}\mathbf{K}_k + \mathbf{R} + \mathbf{P})$$
$$g = 2\left({\mathbf{K}_k}^T \mathbf{Q}^T(\tilde{Y}_k - W_{k+1}) + \mathbf{P}^T U_k\right) \tag{13}$$

the optimal control input correction u_{k+1} yields:

$$u_{k+1} = -\mathbf{H}^{-1} \cdot g \tag{14}$$

Finally, the absolute control input is calculated by

$$U_{k+1_{opt}} = U_k + u_{k+1} \tag{15}$$

3.4 Guideline for Controller Tuning

$\mathbf{Q}, \mathbf{R}$ and $\mathbf{P}$ have to be semi-positive definite in case of the convex formulation (11). In order to obtain a reasonable and stable control the existence of a minimum of (11) has to be guaranteed. For this reason the entries of $\mathbf{Q}, \mathbf{R}$ have to be set in such a way that $\mathbf{H} > 0$ is fulfilled ($\mathbf{P}$ is optional). In general, the adjustment of $\mathbf{Q}, \mathbf{R}$ and $\mathbf{P}$ is intuitive if all considered inputs and outputs of the model are normalized to one in order to have a mutual neutral behaviour in the cost function J. In practice, such normalization for all operating points sometimes is impossible, and the adjustment of the entries in $\mathbf{Q}, \mathbf{R}$ and $\mathbf{P}$ is rather time-consuming. In this case, the penalizing factors adopt the additional function of normalization. This fact has to be considered when finding a good set for $\mathbf{Q}, \mathbf{R}$ and $\mathbf{P}$.

The minimization of dpmax could be switched on by setting the associated entry in the matrix $\mathbf{Q}$ to a value $q_{pmax} > 0$:

$$\mathbf{Q} = \begin{bmatrix} q_{CA50} & 0 & 0 \\ 0 & q_{IMEP} & 0 \\ 0 & 0 & q_{dpmax} \end{bmatrix} \tag{16}$$

The same procedure has to be done to penalize high FMIs with $p_{FMI} > 0$ in the matrix $\mathbf{P}$ for the absolute control inputs:

$$\mathbf{P} = \begin{bmatrix} p_{FMI} & 0 & 0 \\ 0 & p_{SOI} & 0 \\ 0 & 0 & p_{X_{EGR}} \end{bmatrix} \quad , \quad p_{SOI} = p_{X_{EGR}} = 0 \tag{17}$$

To avoid high oscillations in the control inputs or in the worst case an unstable closed loop, the control input corrections u_{k+1} have to be restricted by $\mathbf{R}$:

$$\mathbf{R} = \begin{bmatrix} r_{FMI} & 0 & 0 \\ 0 & r_{SOI} & 0 \\ 0 & 0 & r_{X_{EGR}} \end{bmatrix} \tag{18}$$

For the initial offline controller tuning in case of a normalized controller model, it is practical to set q_{CA50} and q_{IMEP} in $\mathbf{Q}$ equal to one and the entries of $\mathbf{R}$ to about $\frac{1}{10}...\frac{1}{3}$. Hence, for small control errors $\tilde{Y}_{k+1} - W_{k+1}$ a steady state control error can be avoided (because of the lower penalization of the control input corrections u_{k+1}). The entries of $\mathbf{P}$ and q_{dpmax} in $\mathbf{Q}$ are set to zero for the beginning. When this control works fine, p_{FMI} can be slightly increased. Since the absolute value FMI is penalized here, p_{FMI} always has to be lower than the corresponding entry r_{FMI} in $\mathbf{R}$ to avoid over-penalizing for positive corrections of FMI. The fine-tuning of the controller can be performed online. To minimize dpmax and to avoid a permanent high control error in this control output, the corresponding reference value in W_{k+1} is always set slightly lower than its actual measurement, until a physically reasonable minimum is reached. So, an appropriate q_{dpmax} depends on the chosen constant difference between the measurement and the setpoint of dpmax. In analogy to p_{FMI}, q_{dpmax} has to be set to low values for the beginning.

4. RESULTS

The controller is implemented in Matlab/Simulink® and is validated by closed-loop simulations. The model of the plant differs from the model used as internal model of the controller structure. In contrast to the successively updated static controller model, the plant model consists of a series connection of linear dynamic lag elements of first order and the nonlinear artificial neural network. Moreover, the parameters of the ANN are slightly altered and a white noise signal is added to the outputs. Fig. 8 shows some control results of three differently parametrized controllers: 1.) standard controller without penalization of FMI and dpmax $q_{CA50} = 0.5, q_{IMEP} = 2.7, q_{dpmax} = 0, r_{FMI} = 0.08, r_{SOI} = 0.08, r_{X_{EGR}} = 0.16, p_{FMI,SOI,X_{EGR}} = 0$, 2.) with minimization of FMI $p_{FMI} = 0.032$ and 3.) with simultaneous minimization of FMI and dpmax $p_{FMI} = 0.032, q_{dpmax} = 0.05$. In each case, the aim was to follow the steplike changing setpoint in IMEP by simultaneously keeping CA50 constant. The first three plots show the control outputs CA50, IMEP and dpmax. The last three plots show the control inputs SOI, X_{EGR} and FMI. All three controller versions perform this controller task satisfactorily, concerning IMEP and CA50. However, the second controller, with the penalization of high FMI, finds a more intelligent combination of SOI, FMI and X_{EGR}, so that FMI is lower than the FMI calculated by the standard controller for the complete control sequence. 5.13% less fuel is consumed, with respect to the delivered work (integration of the indicated mean effective pressure) and an assumed combustion efficiency $\eta_c = 38\%$, a promising saving of 4% remains. This means a 4% reduction of CO_2-emissions, by assuming a complete combustion for both controller versions. The third controller finds a compromise between a quiet and an efficient engine. It reduces the maximum pressure gradient in combination with lower fuel consumption, as compared to the standard controller. The engine has -13.07% less dpmax than produced by using

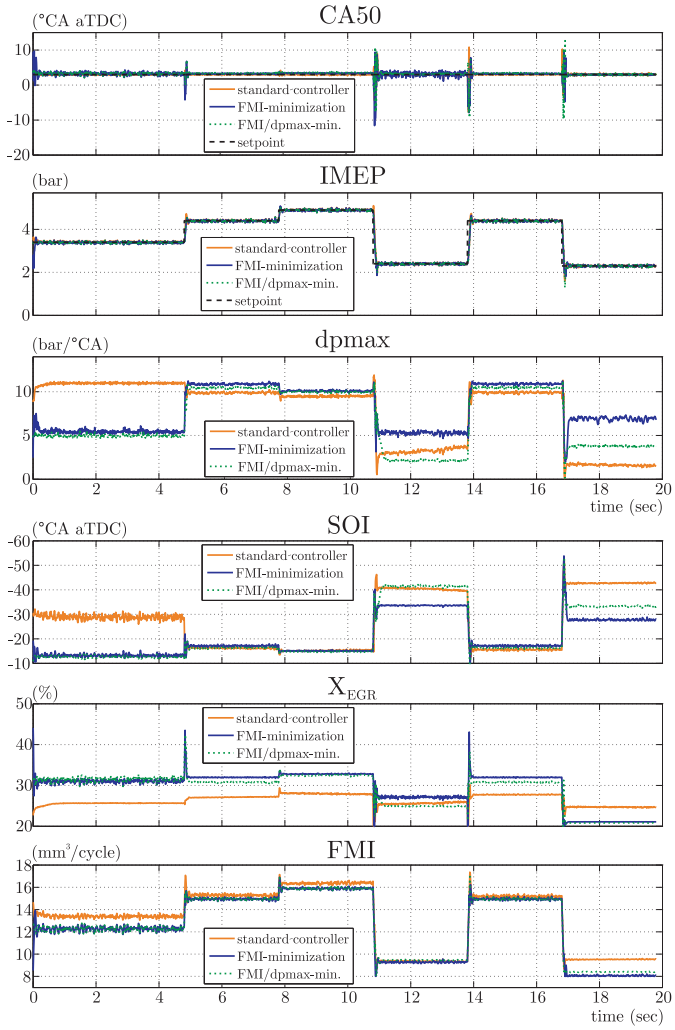

Fig. 8. Comparison of different controller adjustments

the standard controller. All controllers work in the area of PCCI combustion; especially the standard and the third controller partly use an early SOI< −40 °CA aTDC and 25% <X_{EGR} < 33%.

Table 1. Min. FMI and FMI & dpmax vs. standard controller 1)

Minimization	dpmax	fuel	work	real fuel savings
2) FMI	1.13 %	-5.13 %	-0.42 %	4.02 %
3) FMI & dpmax	-13.07 %	-4.47 %	-0.29 %	3.70 %

Table 1 gives an overview of the results for the different controllers, compared to the standard controller for the 20sec control sequence in Fig. 8. The combustion controller was also implemented on a standard Rapid Control Prototyping Hardware for use at the engine test bench. The computational burden is very moderate, it can be calculated under real-time conditions.

5. CONCLUSION

PCCI is a modern clean combustion method, which has a very high potential in reduction of pollutants, like soot and NO_X. To realize this combustion, a model-based optimal controller is presented, which is capable of managing classical combustion parameters, like the indicated mean effective pressure or the position of the combustion average, considering minimization of the fuel consumption. It has been shown that an intelligent combination of the control inputs, the quantity of injected fuel, the start of injection, and the fraction of recirculated exhaust gas can contribute to reduction of fuel consumption of approximately 4%. Moreover, the maximum cylinder pressure gradient, which is responsible for the combustion noise, could be decreased. The presented controller structure demands little in the way of calculation capacity, since no observer is used, and the high, almost proportional, dynamics of the process are neglected in the internal controller model.

ACKNOWLEDGEMENTS

The authors gratefully acknowledge the contribution of the Collaborative Research Centre 686 "Model-based control of homogenized low-temperature combustion" supported by the German Research Foundation (DFG) at RWTH Aachen University, Germany, and Bielefeld University, Germany, see www.sfb686.rwth-aachen.de for details.

REFERENCES

Bengtsson, J., Strandh, P., Johansson, R., Tunestal, P., and Johansson, B. (2006). Multi-output control of a heavy-duty hcci engine using variable valve actuation and model predictive control. *SAE 2006-01-0873*.

Boyd, S. and Vandenberghe, L. (2004). *Convex Optimization*. Cambridge University Press.

Dec, J.E. (2009). Advanced compression-ignition engines understanding the in cylinder processes. *Proceedings of the Combustion Institute*, 32, 2727–2742.

Drews, P., Albin, T., Hoffmann, K., Vanegas, A., Felsch, C., Peters, N., and Abel, D. (2010). Model-based optimal control for pcci combustion engines. *IFAC-Symposium Advances in Automotive Control, Munich, Germany*.

Drews, P., Hoffmann, K., Beck, R., Gasper, R., Vanegas, A., Felsch, C., Peters, N., and Abel, D. (2009). Fast model predictive control for the air path of a turbocharged diesel engine. *Proceedings of the European Control Conference 2009, Budapest, Hungary*, 3377–3382.

Kanda, T., Hakozaki, T., Uchimoto, T., Hatano, J., Kitayama, N., and Sono, H. (2005). PCCI operation with early injection of conventional diesel fuel. *SAE paper 2005-01-0378*.

Kim, M.Y. and Lee, C.S. (2007). Effect of a narrow fuel spray angle and a dual injection configuration on the improvement of exhaust emissions in a hcci diesel engine. *Fuel*, 86, 2871–2880.

Mollenhauer, K. and Tschoeke, H. (2007). *Handbook of Diesel Engines*. Springer.

Shaver, G.M. (2009). Stability analysis of residual-affected hcci using convex optimization. *Control Engineering Practice*, 17, 1454 – 1460.

Yao, M., Zheng, Z., and Liu, H. (2009). Progress and recent trends in homogeneous charge compression ignition (HCCI) engines. *Progress in Energy and Combustion Science*, 35, 398–437.